Observation of the Oxygen Diffusion Barrier in Soybean (*Glycine max*) Nodules with Magnetic Resonance Microscopy

ABSTRACT

The effects of selected gas perfusion treatments on the spin-lattice relaxation times (T_1) of the soybean (*Glycine max*) nodule cortex and inner nodule tissue were studied with ^1H high resolution magnetic resonance microscopy. Three gas treatments were used: (a) perfusion with O_2 followed by N_2; (b) O_2 followed by O_2; and (c) air followed by N_2. Soybean plants with intact attached nodules were placed into the bore of a superconducting magnet and a selected root with nodules was perfused with the gas of interest. Magnetic resonance images were acquired with repetition times from 50 to 3200 ms. The method of partial saturation was used to calculate T_1 times on selected regions of the image. Calculated images based on T_1 showed longer T_1 values in the cortex than in the inner nodule during all of the gas perfusions. When nodules were perfused with O_2-O_2, there was no significant change in the T_1 of the nodule between the two gas treatments. When the nodule was perfused with O_2-N_2 or air-N_2, however, the T_1 of both the cortex and inner nodule increased. In these experiments, the increase in T_1 of the cortex was 2- to 3-fold greater than the increase observed in the inner nodule. A similar change in T_1 was found in detached live nodules, but there was no change in T_1 with selective gas perfusion of detached dead nodules. These observations suggest that cortical cells respond differently to selected gas perfusion than the inner nodule, with the boundary of T_1 change sharply delineated at the interface of the inner nodule and the inner cortex.

Nitrogen fixation in nodules of leguminous plants formed by the symbiotic association of the plant root and N_2-fixing bacteria has been an area of increasing interest. The benefits to the plant of N_2 fixation have become increasingly important as research interests have focused on techniques of low-input, sustainable agriculture.

Several gases play key roles in the process of N_2 fixation, including CO_2, H_2, N_2, and O_2 (15). Each plays a unique and key role in providing energy and substrates for N_2 conversion to the NH_3 necessary for plant assimilation. Regulation of gas, particularly O_2, diffusion through the nodule cortex into the inner nodule and to the bacterioids must meet several requirements. Bacterial N_2 fixation requires large amounts of O_2 for oxidative phosphorylation, providing ATP for activation of the iron- and molybdenum-containing nitrogenase enzyme complex, redox potentials for N_2 fixation, and orientation of the nitrogenase enzyme complex for activity (19, 23, 32). This process is complicated, however, by both reversible and irreversible inhibition of nitrogenase by exposure to free molecular O_2 and by the inhibition of nitrogenase synthesis by O_2. This delicate balance in the regulation of O_2 concentration and flux has been the focus of many investigators (5, 6, 9, 10, 13, 16, 24–26, 28–30).

^1H magnetic resonance microscopy allows the repeated, nondestructive study of intact plants, including roots, stems, and nodules. Due to the noninvasive nature of the technique, the same material can be repeatedly observed under different treatment or experimental conditions (3, 12, 14). Detailed structural information as well as T_1[1] and T_2 relaxation times can be repeatedly acquired on the same specimen, providing the ability to nondestructively test for specific treatment effects. Tissue characteristics such as T_1 and T_2 reflect the degree of proton mobility and exchange within the tissue (18).

The objectives of the current study were to observe and describe the O_2 diffusion barrier through measurement of ^1H (from H_2O) T_1 values within nodules and changes in these values as a function of exposure to specific gases (O_2, ambient air, and N_2).

MATERIALS AND METHODS

Soybean plants (*Glycine max* [L.] Merr. cv Williams) inoculated with *Bradyrhizobium japonicum* USDA 110 or 138 were grown in the growth chamber for approximately 7 weeks. During this period, they received light from fluorescent and incandescent lamps for a photoperiod of 15 h and were exposed to day/night temperatures of 25/19°C and day/night humidity of 80/95%. Plants were irrigated with a nutrient solution containing 1 mM NO_3 and 2 mM Pi (22). During the last 12 to 14 d of growth, the concentration of Pi was raised to 10 mM.

Plants were hand carried or sent by overnight express delivery from the USDA Eastern Regional Laboratory in Philadelphia, PA, to Duke University Medical Center in Durham, NC. Immediately prior to analysis, the plants were carefully removed from their containers and the roots were gently washed free of adhering potting mix. One root with several nodules or nodule clusters was selected. Nodules were selected on the basis of color, size, and turgidity. Only nodules and roots that appeared healthy were selected. The

[1] Abbreviations: T_1, spin-lattice relaxation time; T_2, spin-spin relaxation time; rf, radiofrequency; TR, repetition time; TE, echo time.

selected root with attached nodules was placed into a plastic tube and surrounded within the tube either by moist Ottawa sand (20–30 mesh) or moistened glass wool. At least one small plastic tube containing a solution of $CuSO_4$ was placed parallel to the root to serve as a reference for measurements during the course of the experiment. The root extended from one end of the plastic tube and a Tygon tube was attached to the other end of the root/nodule-containing tube (Fig. 1). The remainder of the root system was carefully wrapped in moist paper towels and placed in a plastic bag to prevent desiccation. The top of the plant was also moistened and wrapped loosely with damp paper towels and plastic.

The tube containing the roots and nodules was carefully placed inside an rf coil. The plant top extended from one end of the rf coil, and the Tygon tube extended from the other end. This apparatus was placed inside the bore of a superconducting magnet, which was part of a GE CSI Imager for Magnetic Resonance Imaging (Fremont, CA). The Tygon tube was attached to a gas tank. Choice of gas was dependent on the particular experiment. Most of the experiments were performed on a 2 T imaging system; however, one additional experiment (O_2-N_2) was performed at 7 T to achieve greater resolution. Gas flowed from a pressure tank into the nodule container, perfusing the nodule and root with the gas of interest at a flow rate of approximately 0.5 L/min.

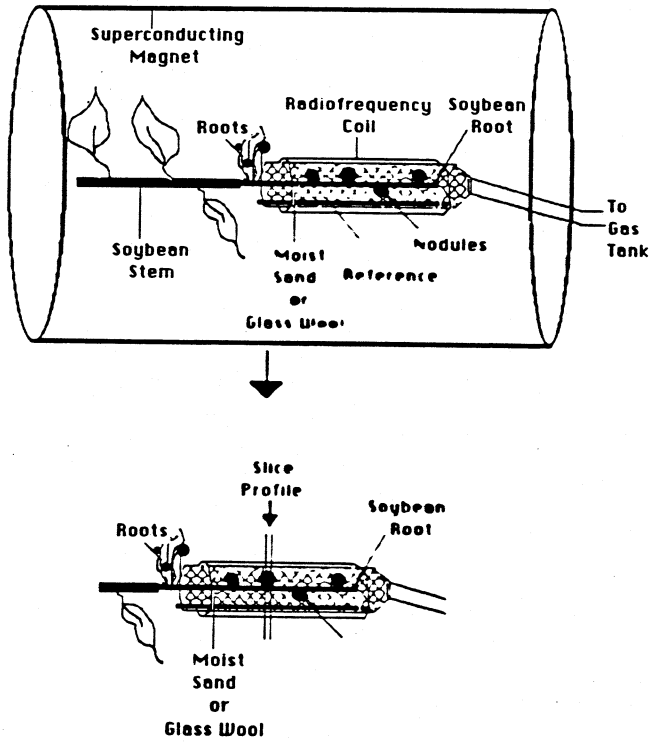

Figure 1. Diagramatic representation of the experimental design and basic equipment used in acquisition of magnetic resonance images of soybean nodules undergoing selective gas perfusions. The rf coil containing the plant roots and nodules is placed into the bore of the superconducting magnet. Roots outside the rf coil and the top of the plant were wrapped in damp paper towels and placed into a plastic bag to reduce desiccation. A slice was selected through the root and nodule (the slice profile), which was repeatedly imaged during the course of the experiment.

Following placement in the magnet bore, cross-sectional locator spin echo images (TR = 100–300 ms, TE = 10 ms) were acquired through the root, nodules, and reference tube. When a nodule was located, a slice profile through the nodule, root, and reference tube was selected with a slice thickness varying between 0.5 and 1.0 mm. Six images were sequentially acquired through the selected slice plane with TR values from 50 to 3200 ms. Total imaging time for acquisition of a set of images required for the calculation of T_1 values was 2 h. Images were acquired and displayed as a 256 × 256 pixel array. Resolution was 30 to 60 μm, depending on the particular experiment. Whenever possible, multi-slice acquisitions were made, allowing measurements on multiple nodules of a single plant. When multi-slice acquisitions were used, a gap equal to or greater than one slice thickness was left between slices. The acquired digital images were then viewed with a Sun Workstation (Sun Microsystems, Mountain View, CA). T_1 values were calculated by the partial saturation method, fitting for pseudo-density, flip angle, and T_1 (18).

For nodules attached to intact plants, gas-perfusion treatments included O_2-O_2 (three plants, eight nodules), O_2-N_2 (five plants, seven nodules), and air-N_2 (three plants, seven nodules). All of the other experiments were done at 2 T, except for one of the O_2-N_2 plants, containing one nodule, which was imaged at 7 T. Measurements on this nodule were not included in the statistical analysis. In addition, nodules were carefully detached from several plants. Half of the nodules were rapidly frozen in liquid N_2 to kill them, then thawed at room temperature. Live and dead nodules were placed together in the rf coil, separated by a divider placed in the center of the tube, then perfused with O_2, followed by N_2. T_1 measurements were made on two of the live and three of the dead nodules during both of the two gas-perfusion treatments.

For each of the perfusion treatments, the nodules were exposed to the first gas for 0.5 to 1.5 h before initiation of the first T_1 image acquisition series. Perfusion by the first gas was maintained during the 2-h image acquisition period. Nodules were then perfused for 2 h with the second gas before initiation of the second T_1 image acquisition series. Perfusion by the second gas also continued during the second image acquisition series.

Relaxation time measurements were first made for selected regions of interest in the images of the T_1 image acquisition series. Measurements were made for the cortex, inner nodule, and reference tube(s) for each nodule/gas perfusion combination. Measurements were made on all imaged nodules. The correlation coefficient (r^2) calculated for each fitted line and data set was ≥ 0.94. T_1 measurements were also made for the reference tube(s) within each image as well as for the cortical and inner regions of each nodule. T_1 values used in the analyses were taken from values calculated from the fitting techniques on the specific regions of interest within each T_1 image set. Measurements for nodule T_1 values were normalized according to the T_1 values calculated for the reference tube(s). This was done by comparing the calculated T_1 value of the reference tube(s) during the two gas-perfusion treat-

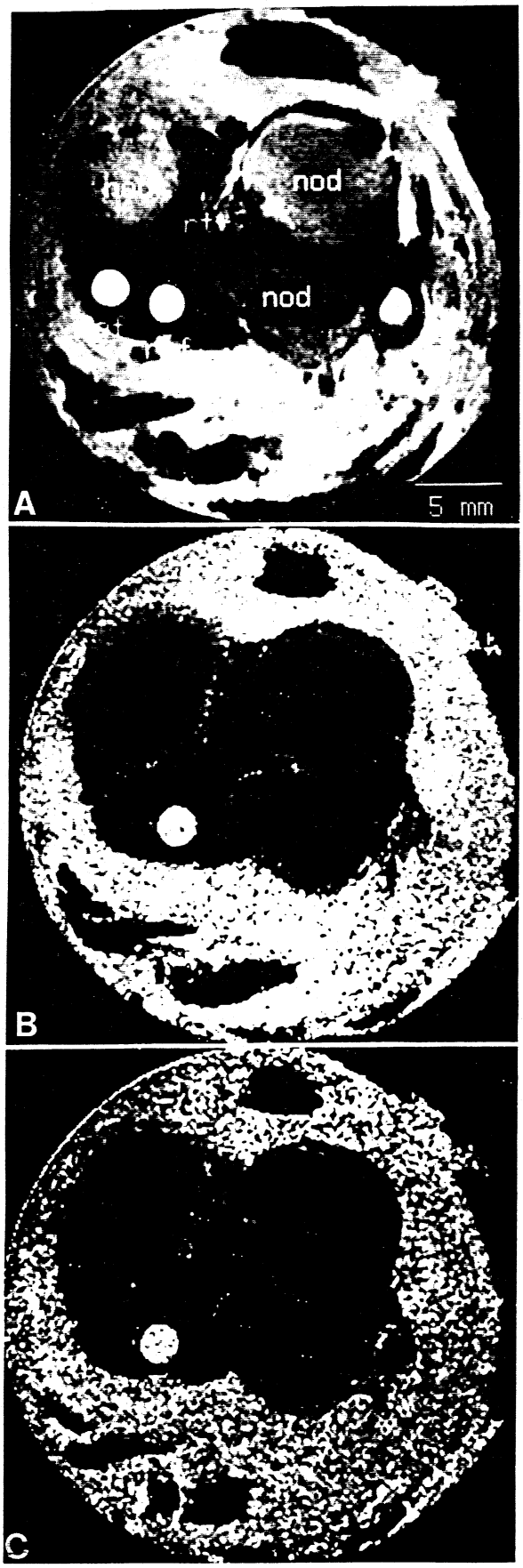

ments. A correction factor was calculated, which, when multiplied by the T_1 for the second perfusion treatment, made it equal to the T_1 for the first gas treatment. In all experiments, the change in the reference T_1 value was less than or equal to 8%. Calculated T_1 values for the nodule during the second gas exposure were also multiplied by this correction factor. Calculated T_1 images were also generated, in which the T_1 value for each pixel in the image was calculated to confirm the pattern of T_1 distribution within each nodule. Calculated images were made for each nodule exposed to each gas (17, 18).

The change in relaxation time between exposure to the first and second gas treatment was measured and tested for significance by a paired *t* test with an estimate for covariance. Differences between the change in relaxation times for specific nodule regions (cortex and inner nodule) and between gas-perfusion experiments (O_2-O_2, O_2-N_2, air-N_2) were tested by analysis of variance.

Self-diffusion coefficients for water were also measured for five replicate nodules perfused with O_2 only. Field strength gradients of varied magnitudes were applied across the slice plane. Signal reduction of specific image regions with increasing gradient strength was fit through an interactive fitting procedure for calculation of diffusion coefficients (mm^2/s) and pseudodensity (27).

RESULTS

Significant structural detail could be observed in nodule images, with the cortex clearly distinguishable from the inner nodule (Figs. 2 and 3). The cortex could be seen as two layers around the nodule perimeter in some of the images. Also, in a few of the images, the inner nodule showed a gradation of signal intensity from the outer boundaries to the center.

The T_1 calculated images clearly showed patterns of differential T_1 values within the nodule tissue (Fig. 2). Signal intensities in the T_1 calculated images directly and quantitatively show the T_1 distribution within the nodule, with the signal intensity (brightness) of the pixel in the calculated image directly proportional to the T_1 (ms). The T_1 values within the nodule cortex were greater than the T_1 values within the inner nodule and appeared homogeneous throughout the cortex, with a sharp delineation at the cortex/inner nodule interface. The inner nodule generally exhibited a homogeneous T_1 distribution, but in a few of the nodules T_1 was longer in the nodule center (as indicated by a greater

Figure 2. Magnetic resonance images of a cross-sectional view through three soybean nodules and a root. These nodules were subjected to the O_2-O_2 gas-perfusion treatments to serve as control nodules. A, Spin-echo image acquired at TR = 3200 ms, TE = 10 ms, nod, Nodule; ref, reference tube filled with $CuSO_4$ solutions; rt, root. B, T_1 calculated image of nodules undergoing the first gas-perfusion treatment, O_2. The signal intensity of the pixels is directly proportional to T_1 (ms). Therefore, the brighter the pixels, the longer the T_1. C, T_1 calculated image of nodules undergoing the second gas-perfusion treatment, O_2. Note in both sets of calculated images that the T_1 of the cortex is longer than the T_1 of the inner nodule (brighter cortex), but there is no change in T_1 with the two gas-perfusion treatments.

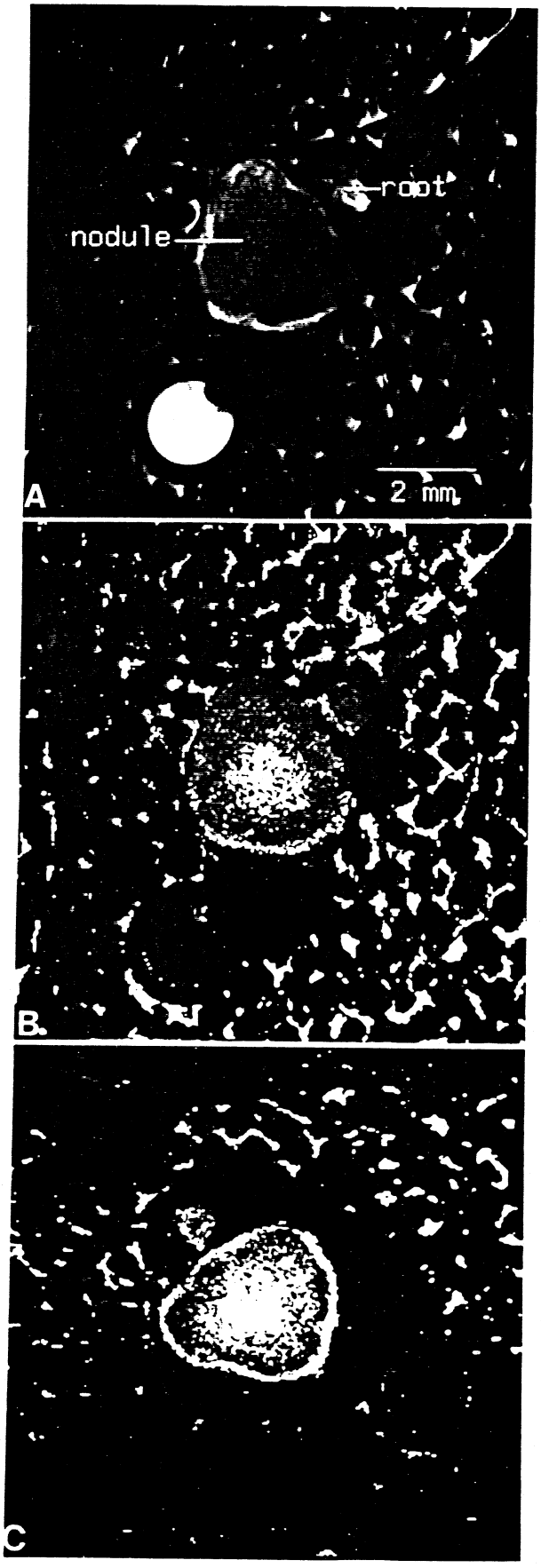

Table I. *Change in T_1 of Soybean (G. max) Nodule Cortex and Inner Nodule following Selective Gas Perfusion*

Treatment groups followed by the same letter are not significantly different at a = 0.05, as determined by protected LSD. Treatments followed by an asterisk (*) have a significant change in T_1 between gas-perfusion treatments at a = 0.05, as determined by a paired *t* test.

Treatment	Change in T_1
	ms
Intact, attached nodules	
O_2-O_2	
Cortex	−58 ± 151a
Inner nodule	−37 ± 32a
C_2-N_2	
Cortex	654 ± 148b*
Inner nodule	304 ± 218c*
Air-N_2	
Cortex	604 ± 351b*
Inner nodule	202 ± 128c*
Detached nodules (O_2-N_2)	
Live nodules	
Cortex	698 ± 19b*
Inner nodule	253 ± 9c*
Dead nodules	
Cortex	−14 ± 43a
Inner nodule	−16 ± 29a

signal intensity in the T_1 calculated images), with a steep gradient of decreasing T_1 values going from the center toward the cortex (Fig. 3B). The greater T_1 observed in the center with some nodules is likely related to nodule age, with heterogeneity in the nodule center reflective of slight nodule senescence. When these nodules were examined following the gas-perfusion experiments, often there was a slight gray cast to the tissue at the center of the inner nodule. The greater T_1 in the nodule center of these few nodules did not change their relaxation time response to the gas treatments, however.

Changes in the relaxation times of the nodules were compared by subtraction of the two T_1 values calculated from data acquired during the two gas-perfusion treatments. For the control nodules that received the O_2-O_2 treatment, there was a small statistically insignificant decrease in the T_1 values measured for both the cortex and the inner nodule (Table I, Fig. 2).

In contrast, the calculated/T_1 for both the cortex and the inner nodule increased significantly in intact, attached nodules with exposure to either air or O_2 followed by N_2 (Table

Figure 3. Magnetic resonance images of a cross-sectional view through a soybean nodule and root. These nodules were subjected to the O_2-N_2 gas-perfusion treatments. A, Spin-echo image acquired at TR = 3200 ms, TE = 10 ms. The large bright tube in the left lower corner is a reference tube filled with $CuSO_4$ solution. B, T_1 calculated image of the nodule, root, and reference tube during the initial gas perfusion with O_2. C, T_1 calculated image of the nodule, root, and reference tube during the second gas-perfusion treatment with N_2. Note the brightness of the cortex under N_2 perfusion compared with the O_2 perfusion, indicating an increase in T_1 with exposure to N_2.

the cortex, regulating O_2 diffusion into the O_2-sensitive inner nodule.

In biological material, the observed relaxation times are a function of the relaxtivity of the components of the system that are in rapid exchange (1, 7). The reciprocal of the measured T_1 is the weighted sum of the reciprocals of the proton sources contributing to the signal. This relationship is described:

$$\frac{1}{T_{1obs}} = \frac{a}{T_{1A}} + \frac{b}{T_{1B}} + \frac{c}{T_{1C}} \cdots$$

where T_{1obs} is the observed T_1; a, b, c . . . are the proportions of each component contributing to the observed signal; and T_{1A}, T_{1B}, T_{1C} . . . are the T_1 values of each component contributing to the observed signal.

In a simple model, it is proposed that there are two main water compartments in exchange, intracellular water and extracellular water, which is in association with a glycoprotein. The intracellular T_1 for highly hydrated tissues such as a soybean nodule has been described as being relatively long (1). Water associated with a viscous, hydrophilic glycoprotein would be expected have a significantly shorter T_1. A similar relationship can be seen in the decrease in T_1 with increasing additions of PEG to water (Fig. 4). Based on the concept of the water in association with a glycoprotein having a short T_1, the change in T_1 may be explained by a change in the proportion of intercellular water and water in the interstitial spaces in association with the glycoprotein. Under a high-O_2 environment, water would fill the interstitial spaces and swell the glycoprotein, occluding channels for O_2 diffusion and restricting O_2 movement into the nodule interior. When exposed to a low O_2 environment, the proportion of short-T_1 water in association with the glycoprotein is decreased either through water movement into the cells or through rapid degradation of the glycoprotein. Either of these mechanisms would open channels for O_2 diffusion and passage to the inner nodule. Both water movement into the cell or rapid glycoprotein degradation would reduce the proportion of short-T_1 water in association with the glycoprotein, increasing the T_1 time of the tissue.

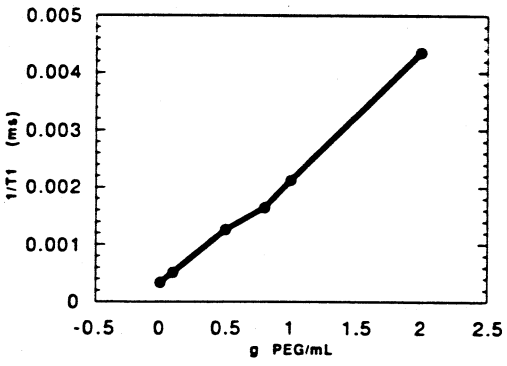

Figure 4. Changes in T_1 of a solution of PEG in water. Increasing amounts of PEG were added to 10 mL of water. Tubes containing the PEG solutions were simultaneously imaged in six images with TR = 100 to 3200 ms. T_1 was calculated by the method of partial saturation (18).

The hypothesis of the change in T_1 being caused by a repartitioning of water between relatively high and low T_1 compartments is also supported by the greater diffusion coefficient calculated for the cortex and compared with the inner nodule. The difference in diffusion coefficients between the nodule regions strongly suggests much greater diffusibility and movement of water within the cortex compared with the inner nodule. Further research is needed for determination of the compartmental T_1 values, water mobility, and volumetric measurements and the status of the glycoprotein under rapidly changing gaseous environments.

These observations are in agreement with changes in the relaxation of ^{31}P of soybean nodules presented in the accompanying report (22). The same pattern of increased T_1 of the nodule cortex with N_2 perfusion following perfusion with either O_2 or ambient air was observed with this nucleus. For both nuclei studied, the short T_1 associated with air or O_2 exposure could be associated either with water or PO_4 in a highly viscous environment, such as in association with a glycoprotein. Although mechanisms of relaxation change are unconfirmed at this time, both PO_4 and ^1H NMR relaxation measurements exhibit similar changes in response to selective gas perfusion.

The experiments presented here provide evidence that the nodule cortex and the inner nodule act in unique and different ways when exposed to specific gas-perfusion treatments. The observed change in T_1 in response to changing the gas perfusion from O_2 or air to N_2 was greater in the cortex than in the inner nodule; however, both exhibited a significant increase in T_1. The change in T_1 extended homogeneously through the nodule cortex and was sharply delineated at the inner cortex-inner nodule interface. Additionally, the T_1 change was observed only in live nodules, suggesting a variable, physiologically mediated process regulating gas diffusion through the nodule. Although the mechanism of change is unconfirmed at this time, it is proposed that the T_1 change is (a) in direct response to O_2 acting as a paramagnetic agent, with the T_1 increase occurring as the O_2 concentration decreases with N_2 perfusion; (b) due to the action of other paramagnetic agents; and/or (3) a consequence of a change in the O_2 diffusion pathways through the cortex, perhaps regulated by an occlusion glycoprotein. It is likely that the change in relaxation times for the nodules is a consequence of a combination of these factors. Therefore, further research needs to be done to confirm the mechanism of T_1 change and the relationship to the nodule mechanism controlling gas diffusion.

LITERATURE CITED

1. **Beall PT, Amtey SR, Kasturi SR** (1984) NMR Data Handbook for Biomedical Applications. Pergamon Press, New York
2. **Bloembergen N, Purcell EM, Pound RV** (1948) Relaxation effects in nuclear magnetic resonance absorption. Physiol Rev **73:** 679
3. **Brown JM, Johnson GA, Kramer PJ** (1986) *In vivo* magnetic resonance microscopy of changing water content in *Pelargonium hortorum* roots. Plant Physiol **82:** 1158–1160
4. **Chiarotti G, Cristiani G, Giulotto L** (1955) Proton relaxation in pure liquids and in liquids containing paramagnetic gases in solution. Nuovo Cimento **1:** 863
5. **Criswell JG, Havelka UD, Quebedeaux B, Hardy RWF** (1976)

Adaptation of nitrogen fixation by intact soybean nodules to altered rhizosphere pO_2. Plant Physiol **58:** 622–625

6. **Dakora FD, Atkins CA** (1989) Diffusion of oxygen in relation to structure and function in legume root nodules. Aust J Plant Physiol **16:** 131–140
7. **Fullerton GD, Potter JL, Dornbluth NC** (1982) NMR relaxation of protons in tissues and other macromolecular water solutions. Magn Reson Imaging **1:** 209–228
8. **Gomori JM, Grossman RI, Yu-Ip C, Asakura T** (1987) NMR relaxation times of blood: dependence on field strength, oxidation and cell integrity. J Comput Assisted Tomogr **11:** 684–690
9. **Hunt S, Gaito ST, Layzell DB** (1988) Model of gas exchange and diffusion in legume nodules. Planta **173:** 128–141
10. **Hunt S, King BJ, Canvin DT, Layzell DB** (1987) Steady and nonsteady state gas exchange characteristics of soybean nodules in relation to the oxygen diffusion barrier. Plant Physiol **84:** 164–172
11. **James EK, Sprent JI, Minchin FR, Brewin NJ** (1990) Intercellular location of glycoprotein in soybean nodules: effect of altered rhizosphere oxygen concentration. Plant Cell Environ **14:** 467–476
12. **Johnson GA, Brown JM, Kramer PJ** (1987) Magnetic resonance microscopy of changes in water content in stems of transpiring plants. Proc Natl Acad Sci USA **84:** 2752–2755
13. **King BJ, Hunt S, Weagle GE, Walsh KB, Pottier RH, Canvin DT, Layzell DB** (1983) Regulation of O_2 concentration in soybean nodules observed by *in situ* spectroscopic measurement of leghemoglobin oxygenation. Plant Physiol **87:** 296–299
14. **Kramer PJ, Siedow JN, MacFall JS** (1990) Nuclear magnetic resonance research on plants. *In* Y Hashimoto, N Nonami, PJ Kramer, BR Strain, eds, Measurement Techniques in Plant Science. Academic Press, New York, pp 403–431
15. **Layzell DB, Hunt S, King BJ, Walsh KB, Weagle GE** (1989) A multichannel system for steady-state and continuous measurements of gas exchanges from legume roots and nodules. *In* JG Torrey, LM Winship, eds, Applications of Continuous and Steady-State Methods to Root Biology. Kluwer Academic Publishers, Dordrecht, The Netherlands, pp 2–53
16. **Layzell DB, Hunt S, Palmer GR** (1989) Mechanism of nitrogenase inhibition in soybean nodules. Plant Physiol **92:** 1101–1107
17. **MacFall JR** (1984) Pulse sequence considerations for computed T1, T2 and spin density images. *In* PD Esser, RE Johnston, eds, Technology of Nuclear Magnetic Resonance. Society of Nuclear Medicine, New York, pp 79–96
18. **MacFall JR, Wehrli FW, Greger RK, Johnson GA** (1987) Methodology for the measurement and analysis of relaxation times in proton imaging. Magn Reson Imaging **5:** 209–220
19. **Mortenson LE** (1987) ATP and nitrogen fixation. *In* WR Ullrich, PJ Aparicio, PJ Syrett, F Castillo, eds, Inorganic Nitrogen Metabolism. Springer-Verlag, New York, p 295
20. **Olivares J, Bedmar EJ** (1987) Nitrogen fixation in rhizobium. Some general features. *In* WR Ullrich, PJ Aparicio, PJ Syrett, F Castillo, eds, Inorganic Nitrogen Metabolism. Springer-Verlag, New York, p 295
21. **Partain CL, James AE, Rollo FD, Price RR** (1983) Nuclear Magnetic Resonance NMR Imaging. WB Saunders, Philadelphia, p 552
22. **Pfeffer PE, Rolin D, Kumosinski TF, MacFall J, Schmidt JH** (1992) ^{31}P relaxation responses associated with N_2/O_2 diffusion in soybean nodule cortical cells and excised cortical tissue. Plant Physiol **100:** 1682–1690
23. **Robertson JG, Farnden KFF** (1980) Ultrastructure and metabolism of the developing legume root nodule. *In* BJ Miflin, ed, The Biochemistry of Plants, Vol 5. Academic Press, New York, pp 65–113
24. **Sheehy JE, Minchin FR, Witty JF** (1983) Biological control of the resistance to oxygen flux in nodules. Ann Bot **52:** 565–571
25. **Sheehy JE, Minchin RF, Witty JF** (1985) Control of nitrogen fixation in a legume nodule: an analysis of the role of oxygen diffusion in relation to nodule structure. Ann Bot **55:** 549–562
26. **Sinclair TR, Goudriaan J** (1981) Physical and morphological constraints on transport in nodules. Plant Physiol **67:** 143–145
27. **Stejskal EO, Tanner JE** (1965) Spin diffusion measurements: spin echoes in the presence of a time-dependent field gradient. J Chem Phys **42:** 288–292
28. **Weisz PR, Sinclair TR** (1987) Regulation of soybean nitrogen fixation in response to rhizosphere oxygen. Plant Physiol **84:** 900–905
29. **Wittenberg JB, Bergersen FJ, Appleby CA, Turner GL** (1974) Facilitated oxygen diffusion. The role of leghemoglobin in nitrogen fixation by bacteroids isolated from soybean root nodules. J Biol Chem **249:** 4057–4066
30. **Witty JF, Minchin RF, Skot L, Sheehy JE** (1986) Nitrogen fixation and oxygen in legume root nodules. Oxf Surv Plant Mol Cell Biol **3:** 255–314
31. **Witty JF, Skot L, Revsbech NP** (1987) Direct evidence for changes in the resistance of legume root nodules to O_2 diffusion. J Exp Bot **38:** 1129–1140
32. **Yates MG** (1980) Biochemistry of nitrogen fixation. *In* BJ Miflin ed, The Biochemistry of Plants, Vol 5. Academic Press, New York, pp 1–64